Absence of Magnetic Thermal Conductivity in the Quantum Spin-Liquid Candidate $YbMgGaO_4$

Y. Xu,[1] J. Zhang,[1] Y. S. Li,[2,3] Y. J. Yu,[1] X. C. Hong,[1] Q. M. Zhang,[2,4,5] and S. Y. Li[1,5,*]

[1]*State Key Laboratory of Surface Physics, Department of Physics, and Laboratory of Advanced Materials, Fudan University, Shanghai 200433, China*

[2]*Department of Physics, Renmin University of China, Beijing 100872, China*

[3]*Experimental Physics VI, Center for Electronic Correlations and Magnetism, University of Augsburg, 86159 Augsburg, Germany*

[4]*Department of Physics and Astronomy, Shanghai Jiao Tong University, Shanghai 200240, China*

[5]*Collaborative Innovation Center of Advanced Microstructures, Nanjing 210093, China*

(Received 24 October 2016; revised manuscript received 17 November 2016; published 23 December 2016)

We present the ultralow-temperature specific heat and thermal conductivity measurements on single crystals of $YbMgGaO_4$, which was recently argued to be a promising candidate for a quantum spin liquid (QSL). In a zero magnetic field, a large magnetic contribution of specific heat is observed, and exhibits a power-law temperature dependence ($C_m \sim T^{0.74}$). On the contrary, we do not observe any significant contribution of thermal conductivity from magnetic excitations. In magnetic fields $H \geq 6$ T, the exponential T dependence of C_m and the enhanced thermal conductivity indicate a magnon gap of the fully polarized state. The absence of magnetic thermal conductivity at the zero field in this QSL candidate puts a strong constraint on the theories of its ground state.

DOI: 10.1103/PhysRevLett.117.267202

The notion of a quantum spin liquid (QSL) reentered the view of researchers in 1987 [1], fourteen years after it was first proposed by Anderson when he tackled the possibility of a peculiar destruction of magnetism exhibited by spins in a triangular lattice [2]. Ever since then, the passion for searching candidate materials that may harbor such an exotic state of matter has never cooled down [3–17]. In a QSL, a macroscopic number of spins are entangled but can evade symmetry-breaking long-range magnetic order with the help of geometrical frustration, and remain fluidlike even in the zero-temperature limit. Instead of adopting a static arrangement, the spins fluctuate perpetually [18,19].

As the QSL state was firmly established in one-dimensional spin systems [20,21], realizing QSLs in two- and three-dimensional systems has been pursued extensively. Of specific interest has been the spin-1/2 triangular- and kagome-lattice Heisenberg antiferromagnets, in which the former one is the very prototype of a QSL in Anderson's resonating-valence-bond model [1,2,22]. After the wave of research on the star systems like κ-$(BEDT\text{-}TTF)_2Cu_2(CN)_3$ [4–6], $ZnCu_3(OH)_6Cl_2$ [8–13], and $EtMe_3Sb[Pd(dmit)_2]_2$ [14–16], the newly discovered $YbMgGaO_4$ was argued to be a promising candidate for a QSL [23–27]. No indication of magnetic ordering was observed in specific heat measurements on polycrystalline $YbMgGaO_4$ down to 60 mK, far below the Curie-Weiss temperature $\theta_W \approx 4$ K [23]. A broad continuum of spin excitations, which is a hallmark of the QSL state, was observed in neutron scattering measurements, confirming $YbMgGaO_4$ to be a highly promising QSL candidate [26,27]. Furthermore, the ground state of $YbMgGaO_4$ was proposed to be a gapless U(1) QSL with a spinon Fermi surface, which was evidenced by the temperature dependence of the specific heat ($C_m \sim T^{2/3}$) [23,27], the muon spin relaxation (μSR) results [25], and the crucial features in the inelastic neutron scattering spectrum [26]. As for the mechanism to stabilize a QSL ground state on the triangular lattice of $YbMgGaO_4$, there are two potential ones: while the neutron scattering study identifies the next-nearest-neighbor interactions in the presence of planar anisotropy as key ingredients for QSL formation [27], the electron-spin resonance measurement ascribes the QSL physics to the anisotropy of the nearest-neighbor spin interaction due to the strong localization of $4f$ electrons and the weak dipolar interaction [24].

To understand the nature of a QSL, knowledge of the low-lying elementary excitations would be of primary importance. Ultralow-temperature specific heat and thermal conductivity measurements have proven to be powerful means in the study of low-lying excitations in QSL candidates [5,6,15,16]. Although the gapless feature of the low-energy excitations was reported by the specific heat measurement in κ-$(BEDT\text{-}TTF)_2Cu_2(CN)_3$ [5], the thermal conductivity result implied a possibility of a tiny gap opening [6]. In the case of $EtMe_3Sb[Pd(dmit)_2]_2$, both measurements indicated the existence of gapless spin excitations [15,16].

In this Letter, we report the ultralow-temperature specific heat and thermal conductivity measurements on high-quality $YbMgGaO_4$ single crystals. In the zero magnetic field, a large magnetic contribution with a power-law temperature dependence ($C_m \sim T^{0.74}$) is observed in the

specific heat. However, no significant contribution from magnetic excitations is detected in the thermal conductivity. In magnetic fields $H \geq 6$ T, the behaviors of the specific heat and the thermal conductivity are consistent with a fully-polarized state. We discuss the origin of the absence of magnetic thermal conductivity in this QSL candidate.

The high-quality single crystals of $YbMgGaO_4$ used in this Letter, as well as the nonmagnetic isostructural material $LuMgGaO_4$, were grown by the floating zone technique [24]. The specific heat of the $YbMgGaO_4$ single crystal was measured from 0.05 to 3 K in a physical property measurement system (PPMS, Quantum Design) equipped with a small dilution refrigerator. The $YbMgGaO_4$ sample for the thermal conductivity measurements was cut into a rectangular shape of dimensions 2.50×0.81 mm^2 in the ab plane, with a thickness of 0.30 mm along the c axis. Contacts were made directly on the sample surfaces with silver epoxy. An annealing process was conducted at 400 °C for 30 min to gain a better contact. The thermal conductivity was measured in a dilution refrigerator, using a standard four-wire steady-state method with two RuO_2 chip thermometers, calibrated *in situ* against a reference RuO_2 thermometer. Magnetic fields were applied along the c axis for both the specific heat and thermal conductivity measurements. For comparison, the thermal conductivity of the $LuMgGaO_4$ single crystal was also measured on a sample with dimensions of $1.48 \times 0.78 \times 0.31$ mm^3.

Figure 1(a) shows the specific heat of the $YbMgGaO_4$ single crystal at the zero magnetic field $H = 0$ T, which is nearly identical to the data of the polycrystalline sample we measured previously [23]. Figure 1(b) shows the specific heat of the nonmagnetic counterpart $LuMgGaO_4$ polycrystalline sample (data from Ref. [23]). It can be clearly seen that the magnitude of the specific heat of $YbMgGaO_4$ is far beyond that of $LuMgGaO_4$ in our temperature range (0.05–3 K). As described in Ref. [23], the specific heat of $LuMgGaO_4$ well follows the Debye law with a Debye temperature ~151 K. The magnetic specific heat (C_m) of $YbMgGaO_4$ can be extracted by subtracting the lattice contribution, i.e., the specific heat of $LuMgGaO_4$, from that of $YbMgGaO_4$. The C_m of $YbMgGaO_4$ in zero and finite magnetic fields up to 9 T are plotted in Fig. 1(c) in a log-log scale. The feature at the lowest temperatures comes from the Schottky contribution. As seen in Fig. 1(c), the zero-field specific heat of $YbMgGaO_4$ can be well fitted by $C_m = cT^\beta$ with $\beta = 0.74$ (fitting range 0.10–0.65 K). This value coincides with the value reported previously [23,27], and is close to 2/3. As analyzed in Ref. [26], a gapless QSL with a spinon Fermi surface would give a spinon specific heat $C_m \sim T$, which is further corrected to $C_m \sim T^{2/3}$ if there are strong U(1) gauge fluctuations [26].

Although the zero-field specific heat of the $YbMgGaO_4$ single crystal can be fitted into a theoretical framework satisfactorily, the picture is rather complicated under magnetic fields. As seen in Fig. 1(c), the magnetic field

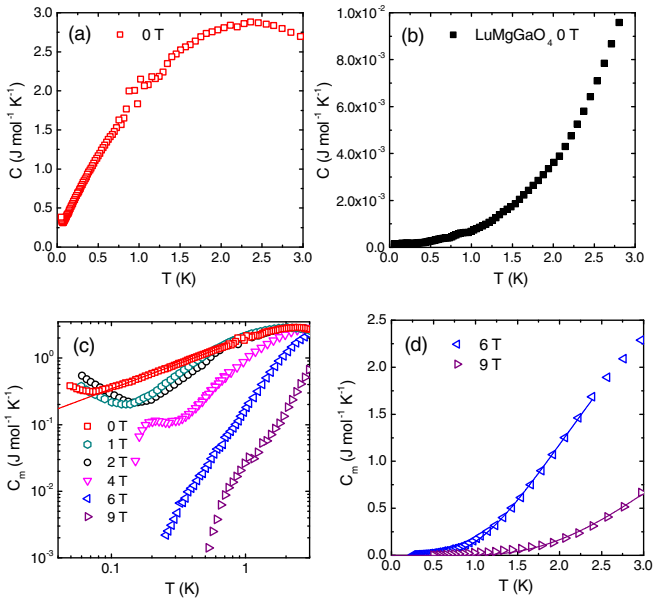

FIG. 1. (a) The specific heat of the $YbMgGaO_4$ single crystal at the zero magnetic field $H = 0$ T. (b) The specific heat of the $LuMgGaO_4$ polycrystalline sample at $H = 0$ T (data from Ref. [23]). (c) The magnetic specific heat of the $YbMgGaO_4$ single crystal at various magnetic fields up to 9 T in a log-log scale. The magnetic specific heat is extracted by subtracting the specific heat of $LuMgGaO_4$ from that of $YbMgGaO_4$. The solid line is the fit of the 0 T data to $C_m = cT^\beta$ between 0.10 and 0.65 K. (d) The specific heat of the $YbMgGaO_4$ single crystal at $H = 6$ and 9 T. The solid lines are the fits to $C_m = de^{-\Delta/k_BT}$, in which Δ is the magnon gap in the fully polarized state.

rapidly suppresses the C_m. Under magnetic fields, the temperature dependence of the C_m gradually turns into an exponential one, as seen in Fig. 1(d). Such an exponential $C_m(T)$ is attributed to the magnons with a gap in a fully polarized state. This fully-polarized state for $YbMgGaO_4$ with very small exchange couplings is evidenced in the magnetization measurements, from which the magnetization tends to saturate above $H = 6$ T in $H \| c$ and $T \sim 2$ K [24,26]. In Fig. 1(d), we fit the 6 T and 9 T data with $C_m = de^{-\Delta/k_BT}$, in which Δ is the magnon gap in the fully polarized state. The fittings give $\Delta = 4.17$ K, $d = 9.50$ J mol^{-1} K^{-1} (fitting range 0.81–2.39 K) and $\Delta = 8.26$ K, $d = 10.4$ J mol^{-1} K^{-1} (fitting range 1.24–2.97 K), respectively. With $J_{\pm\pm} = 0.2J_{zz}$ and a fitting formula from Ref. [28], we calculate the magnon gap Δ to be 0.41 meV (4.69 K) for $H = 6$ T and 0.73 meV (8.40 K) for $H = 9$ T along the c axis. These calculated gap values are a good match with the fitted ones from our specific heat data.

Thermal conductivity measurement is highly advantageous in probing the elementary excitations in QSL candidates, since it is only sensitive to itinerant excitations and is not complicated by the Schottky contribution as observed in the specific heat measurement [6,29]. Figure 2(a) shows the in-plane thermal conductivity of the $YbMgGaO_4$ single crystal at $H = 0$ T. For comparison, the in-plane thermal

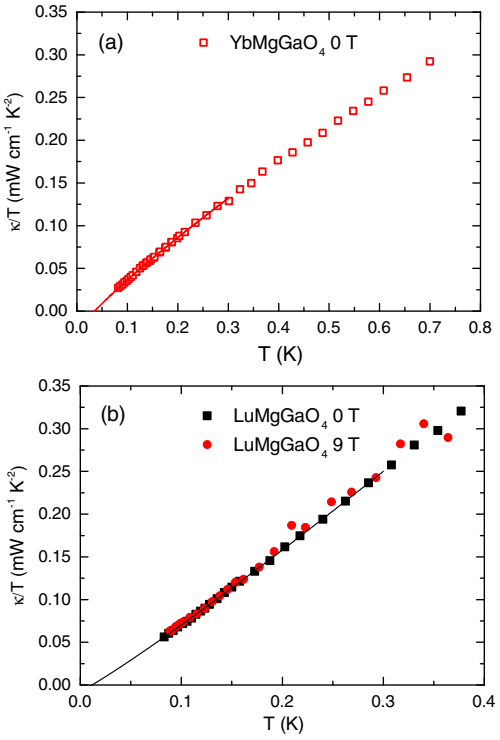

FIG. 2. The in-plane thermal conductivity of (a) the $YbMgGaO_4$ single crystal at $H = 0$ T and (b) the $LuMgGaO_4$ single crystal at $H = 0$ and 9 T. The solid lines are the fits to the data below 0.3 K to $\kappa/T = a + bT^{\alpha-1}$. Note that the applying of a 9 T magnetic field has no effect on the thermal conductivity of nonmagnetic $LuMgGaO_4$.

conductivity of the nonmagnetic counterpart $LuMgGaO_4$ single crystal at $H = 0$ T is also plotted in Fig. 2(b). In a solid, the contributions to thermal conductivity may come from various quasiparticles, such as electrons, phonons, magnons, and spinons. For nonmagnetic compounds, the thermal conductivity at very low temperature can usually be fitted to $\kappa = aT + bT^{\alpha}$, in which the two terms aT and bT^{α} represent contributions from electrons and phonons, respectively [30,31]. Because of the specular reflections of phonons at the sample surfaces, the power α in the second term is typically between 2 and 3 [30,31]. The fitting of the data below 0.3 K for $LuMgGaO_4$ gives $\kappa_0/T \equiv a = -0.007 \pm 0.002$ mW K^{-2} cm^{-1}, and $\alpha = 2.09 \pm 0.02$. Comparing with our experimental error bar ± 0.005 mW K^{-2} cm^{-1}, the κ_0/T of $LuMgGaO_4$ at zero field is virtually zero. This is reasonable, since $LuMgGaO_4$ is an insulator. For $YbMgGaO_4$ with a triangular lattice of spins, one may expect a significant contribution to thermal conductivity by magnetic excitations due to its large C_m. However, with a first glance at the raw data in Fig. 2(a), the magnitude of its κ is only half of that of $LuMgGaO_4$ in Fig. 2(b), although the two samples have a comparable cross-section area (thus the mean free path of the phonons in the boundary scattering limit). We also fit the zero-field data of $YbMgGaO_4$ below 0.3 K to $\kappa/T = a + bT^{\alpha-1}$, which gives $\kappa_0/T \equiv a = -0.025 \pm 0.002$ mW K^{-2} cm^{-1} and $\alpha = 1.85 \pm 0.02$.

A negative κ_0/T has no physical meaning, and the power α is abnormally lower than 2 for $YbMgGaO_4$. Since the specific heat measurements indicate the existence of a sufficient amount of magnetic excitations in $YbMgGaO_4$, it is reasonable to assume that the phonons are scattered not only by the sample boundaries, but also by these magnetic excitations. To verify this assumption, we examine the thermal conductivity of $YbMgGaO_4$ in magnetic fields up to 9 T, as plotted in Fig. 3(a). While applying a 9 T field has no effect on the κ of nonmagnetic $LuMgGaO_4$, as seen in Fig. 2(b), the field has a significant effect on the κ of $YbMgGaO_4$. Figure 3(b) plots the field dependence of the κ/T at 0.2 K. The κ/T first decreases slightly for $H < 2$ T, then there is a sharp increase (by about 35%) between 2 and 5 T, and it finally saturates for $H > 5$ T. While the magnetic state of $YbMgGaO_4$ in the intermediate fields ($0 < H < 5$ T) is rather complex, it simply tends to become a fully polarized state for $H > 5$ T at such low temperatures, as evidenced by previous magnetization [24,26] and our current specific heat measurements. In the fully-polarized state with a magnon gap of several Kelvins, there are almost no magnetic excitations to scatter

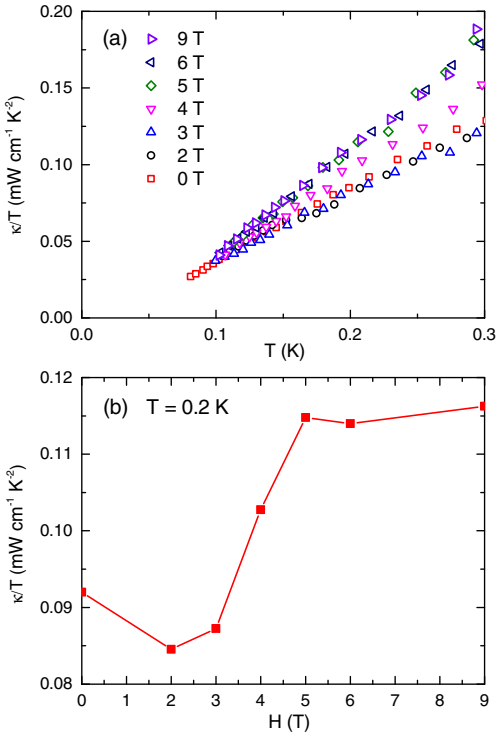

FIG. 3. (a) The in-plane thermal conductivity of the $YbMgGaO_4$ single crystal at various magnetic fields up to 9 T. (b) Field dependence of the κ/T at 0.2 K. The κ/T first decreases slightly for $H < 2$ T, then increases sharply (by about 35%) for 2 T $< H <$ 5 T, and finally saturates for $H > 5$ T. The saturated thermal conductivity above 5 T is purely attributed to phonons, without scattering by magnetic excitations.

phonons below 0.3 K; therefore, the κ of $YbMgGaO_4$ at $H > 5$ T is purely contributed by phonons. Indeed, both the magnitude and the temperature dependence of κ for $YbMgGaO_4$ at $H > 5$ T are more closer to those of $LuMgGaO_4$. At lower fields, it is the additional scattering of phonons by magnetic excitations that suppresses the κ and gives the abnormal temperature dependence of κ and the unphysical negative κ_0/T for $YbMgGaO_4$.

The large C_m and its temperature dependence ($C_m \sim T^{2/3}$) suggest a gapless U(1) QSL with a spinon Fermi surface [26]. Neutron scattering measurement also observed diffusive spin excitations above 0.1 meV, indicating the particle-hole excitation of a spinon Fermi surface [26]. In this context, it is quite surprising that we do not observe any significant magnetic contribution to the κ of $YbMgGaO_4$. By contrast, $EtMe_3Sb[Pd(dmit)_2]_2$ has a κ_0/T as big as 2 $mW\,K^{-2}\,cm^{-1}$ [15]. This means that either (a) the presumed gapless spinons do not exist in $YbMgGaO_4$ and the large C_m has some other magnetic origin, or (b) the gapless spinons do exist but for some reason they do not conduct heat significantly in $YbMgGaO_4$.

In the case that $YbMgGaO_4$ does have a QSL state with gapless spinons, there are two further possibilities. One is that the ground state can be described as a gapless U(1) QSL [24–26]. In this scenario, the low-energy spinons are no longer well-defined Laudau quasiparticles, and the simple kinetic formula is invalid. Note that this may not be true for $YbMgGaO_4$ at $T > 0.1$ K, since the gauge field scattering might only take effect at lower temperatures due to its very low isotropic Heisenberg coupling $J_0 \sim 1.5$ K [24]. Nevertheless, considering the strong U(1) gauge fluctuations, a theoretical formula is derived for a gapless U(1) QSL with a spinon Fermi surface in the clean limit as below [29,32]:

$$\frac{\kappa}{T} = \frac{k_B^2}{\hbar}\left(\frac{\epsilon_F}{k_B T}\right)^{\frac{2}{3}}\frac{1}{d}, \tag{1}$$

where ϵ_F is the spinon Fermi energy, and d is the interlayer distance. Taking $\epsilon_F \approx J_0 \sim 1.5$ K [6,24] and $d = 25$ Å [23], we estimate $\kappa/T \approx 0.044\,mW\,K^{-2}\,cm^{-1}$ at $T = 0.1$ K. This value is even higher than the total κ/T we measured, and there is also no visible $T^{-2/3}$-dependent spinon thermal conductivity κ/T on top of the normal phonon contribution in Fig. 2(a). It is not clear whether the impurity scattering will further reduce this estimation [6,29], and cause the absence of magnetic thermal conductivity in $YbMgGaO_4$. We also notice another calculation of the thermal conductivity for a spinon Fermi surface coupled to a U(1) gauge field, which gives $\kappa/T \approx A_{xx}T^{-1/2+5\epsilon/4} + A_{yy}T^{1/2+3\epsilon/4}$ in an intermediate temperature regime [33,34]. However, if a phonon term $bT^{\alpha-1}$ is added to fit the total κ/T, there are too many parameters for us to make a quantitative analysis.

Another possibility is that the gapless spinons in the QSL ground state of $YbMgGaO_4$ are still well-defined Laudau quasiparticles. Then we try to find out the origin of the absence of spinon thermal conductivity by estimating their mean free path. According to the kinetic formula, the thermal conductivity is written as $\kappa_m = \frac{1}{3}C_m v_F l$, where C_m, v_F and l are the specific heat, Fermi velocity and the mean free path of spinons, respectively. A large C_m and a negligible contribution to thermal conductivity might come from the reduction of v_F or/and l. By comparing Fig. 3(a) (intensity contour plot of spin excitation spectrum along the high-symmetry momentum directions) and Fig. S3b (calculated dynamic spin structure factor along high symmetry points) of Ref. [26], we get $v_F = 1.82 \times 10^2$ m/s. Even if the κ/T at 0.1 K is totally contributed by spinons, l would only be 8.6 Å, about 2.5 times that of the interspin distance (~3.4 Å). For comparison, the gapless excitations have an l as long as ~1000 inter-spin distance in $EtMe_3Sb[Pd(dmit)_2]_2$ [15]. For $EtMe_3Sb[Pd(dmit)_2]_2$, a linear term of $\gamma = 20\,mJ\,K^{-2}\,mol^{-1}$ [16] in the specific heat and a linear term of $\kappa_0/T = 2\,mW\,K^{-2}\,cm^{-1}$ [15] in the thermal conductivity indicate the presence of highly mobile gapless magnetic excitations with an extremely long l. In the case that the gapless spinons do exist in $YbMgGaO_4$, although its C_m is 1 order of magnitude larger than that of $EtMe_3Sb[Pd(dmit)_2]_2$, the small v_F and the extremely short l might be the reason why these spinons do not contribute significantly to the thermal conductivity at the zero magnetic field. One possible mechanism of the spinon localization may be the disorder of Mg^{2+}-Ga^{3+} sites (random occupation) in the double layers of Mg/GaO_5 triangular bipyramids [23].

For another triangular-lattice QSL candidate κ-$(BEDT\text{-}TTF)_2Cu_2(CN)_3$, the specific heat measurement gives a linear term of $\gamma = 15\,mJ\,K^{-2}\,mol^{-1}$ [5]. However, the specific-heat data are plagued by a very large nuclear Schottky contribution below 1 K, which might lead to ambiguity [6]. The magnetic part of the thermal conductivity of κ-$(BEDT\text{-}TTF)_2Cu_2(CN)_3$ exhibits an exponential temperature dependence and gives negligible κ_0/T, which was interpreted as evidence of a gapped QSL [6]. An alternative explanation to reconcile the specific heat and thermal conductivity of κ-$(BEDT\text{-}TTF)_2Cu_2(CN)_3$ is that the gapless spin excitations may be localized due to the inhomogeneity [35]. Here for $YbMgGaO_4$, its ground state apparently cannot be described by the gapped QSL due to the large C_m down to 0.1 K. More low-energy experimental techniques, such as nuclear magnetic resonance, are highly desired to determine whether its ground state is a gapless QSL with localized spinons.

In summary, we have measured the ultralow-temperature specific heat and thermal conductivity of $YbMgGaO_4$ single crystals. The large magnetic specific heat C_m down to 0.1 K and its power-law temperature dependence ($C_m \sim T^{0.74}$) suggest gapless magnetic excitations. The exponential C_m at fields above 6 T indicates a fully polarized state. The thermal conductivity reveals no

significant positive contribution from magnetic excitations. Instead, it is dominated by phonons, and the additional scattering of phonons by magnetic excitations at low fields reduces its value. The absence of magnetic thermal conductivity at zero field in $YbMgGaO_4$ puts a strong constraint on the theories of its ground state.

We thank Shiliang Li, Hong Yao, Weiqiang Yu, and Yi Zhou for helpful discussions. This work is supported by the Ministry of Science and Technology of China (Grants No. 2015CB921401, No. 2016YFA0300503, and No. 2016YFA0300504), the Natural Science Foundation of China, the NSAF (Grant No. U1630248), the Program for Professor of Special Appointment (Eastern Scholar) at Shanghai Institutions of Higher Learning, and STCSM of China (No. 15XD1500200).

*shiyan_li@fudan.edu.cn.

[1] P. W. Anderson, The resonating valence bond state in La_2CuO_4 and superconductivity, Science **235**, 1196 (1987).
[2] P. W. Anderson, Resonating valence bonds: A new kind of insulator?, Mater. Res. Bull. **8**, 153 (1973).
[3] R. Coldea, D. A. Tennant, and Z. Tylczynski, Extended scattering continua characteristic of spin fractionalization in the two-dimensional frustrated quantum magnet Cs_2CuCl_4 observed by neutron scattering, Phys. Rev. B **68**, 134424 (2003).
[4] Y. Shimizu, K. Miyagawa, K. Kanoda, M. Maesato, and G. Saito, Spin-Liquid State in an Organic Mott Insulator with a Triangular Lattice, Phys. Rev. Lett. **91**, 107001 (2003).
[5] S. Yamashita, Y. Nakazawa, M. Oguni, Y. Oshima, H. Nojiri, Y. Shimizu, K. Miyagawa, and K. Kanoda, Thermodynamic properties of a spin-1/2 spin-liquid state in a κ-type organic salt, Nat. Phys. **4**, 459 (2008).
[6] M. Yamashita, N. Nakata, Y. Kasahara, T. Sasaki, N. Yoneyama, N. Kobayashi, S. Fujimoto, T. Shibauchi, and Y. Matsuda, Thermal-transport measurements in a quantum spin-liquid state of the frustrated triangular magnet κ-$(BEDT\text{-}TTF)_2Cu_2(CN)_3$, Nat. Phys. **5**, 44 (2009).
[7] Y. Kurosaki, Y. Shimizu, K. Miyagawa, K. Kanoda, and G. Saito, Mott Transition from a Spin Liquid to a Fermi Liquid in the Spin-Frustrated Organic Conductor κ-$(ET)_2Cu_2(CN)_3$, Phys. Rev. Lett. **95**, 177001 (2005).
[8] M. P. Shores, E. A. Nytko, B. M. Bartlett, and D. G. Nocera, A structurally perfect $S = 1/2$ kagome antiferromagnet, J. Am. Chem. Soc. **127**, 13462 (2005).
[9] B. G. Levi, New candidate emerges for a quantum spin liquid, Phys. Today **60**, 16 (2007).
[10] J. S. Helton *et al.*, Spin Dynamics of the Spin-1/2 Kagome Lattice Antiferromagnet $ZnCu_3(OH)_6Cl_2$, Phys. Rev. Lett. **98**, 107204 (2007).
[11] P. Mendels, F. Bert, M. A. de Vries, A. Olariu, A. Harrison, F. Duc, J. C. Trombe, J. S. Lord, A. Amato, and C. Baines, Quantum Magnetism in the Paratacamite Family: Towards an Ideal Kagome Lattice, Phys. Rev. Lett. **98**, 077204 (2007).
[12] T. H. Han, J. S. Helton, S. Chu, D. G. Nocera, J. A. Rodriguez-Rivera, C. Broholm, and Y. S. Lee, Fractionalized excitations in the spin-liquid state of a kagome-lattice antiferromagnet, Nature (London) **492**, 406 (2012).
[13] M. X. Fu, T. Imai, T. H. Han, and Y. S. Lee, Evidence for a gapped spin-liquid ground state in a kagome Heisenberg antiferromagnet, Science **350**, 655 (2015).
[14] T. Itou, A. Oyamada, S. Maegawa, M. Tamura, and R. Kato, Quantum spin liquid in the spin-1/2 triangular antiferromagnet $EtMe_3Sb[Pd(dmit)_2]_2$, Phys. Rev. B **77**, 104413 (2008).
[15] M. Yamashita, N. Nakata, Y. Senshu, M. Nagata, H. M. Yamamoto, R. Kato, T. Shibauchi, and Y. Matsuda, Highly mobile gapless excitations in a two-dimensional candidate quantum spin liquid, Science **328**, 1246 (2010).
[16] S. Yamashita, T. Yamamoto, Y. Nakazawa, M. Tamura, and R. Kato, Gapless spin liquid of an organic triangular compound evidenced by thermodynamic measurements, Nat. Commun. **2**, 275 (2011).
[17] Y. S. Li, B. Pan, S. Li, W. Tong, L. Ling, Z. Yang, J. Wang, Z. Chen, Z. Wu, and Q. Zhang, Gapless quantum spin liquid in the $S = 1/2$ anisotropic kagome antiferromagnet $ZnCu_3(OH)_6SO_4$, New J. Phys. **16**, 093011 (2014).
[18] P. A. Lee, An end to the drought of quantum spin liquids, Science **321**, 1306 (2008).
[19] L. Balents, Spin liquids in frustrated magnets, Nature (London) **464**, 199 (2010).
[20] D. A. Tennant, T. G. Perring, R. A. Cowley, and S. E. Nagler, Unbound Spinons in the $S = 1/2$ Antiferromagnetic Chain $KCuF_3$, Phys. Rev. Lett. **70**, 4003 (1993).
[21] M. Mourigal, M. Enderle, A. Klopperpieper, J. S. Caux, A. Stunault, and H. M. Ronnow, Fractional spinon excitations in the quantum Heisenberg antiferromagnetic chain, Nat. Phys. **9**, 435 (2013).
[22] G. Baskaran, Z. Zou, and P. W. Anderson, The resonating-valence-bond state and high-T_c superconductivity, Solid State Commun. **63**, 973 (1987).
[23] Y. S. Li, H. Liao, Z. Zhang, S. Li, F. Jin, L. Ling, L. Zhang, Y. Zou, L. Pi, Z. Yang, J. Wang, Z.Wu, and Q. Zhang, Gapless quantum spin-liquid ground state in the two-dimensional spin-1/2 triangular antiferromagnet $YbMgGaO_4$, Sci. Rep. **5**, 16419 (2015).
[24] Y. S. Li, G. Chen, W. Tong, L. Pi, J. Liu, Z. Yang, X. Wang, and Q. Zhang, Rare-Earth Triangular Lattice Spin Liquid: A Single-Crystal Study of $YbMgGaO_4$, Phys. Rev. Lett. **115**, 167203 (2015).
[25] Y. S. Li, D. Adroja, P. K. Biswas, P. J. Baker, Q. Zhang, J. J. Liu, A. A. Tsirlin, P. Gegenwart, and Q. M. Zhang, Muon Spin Relaxation Evidence for the U(1) Quantum Spin-Liquid Ground State in the Triangular Antiferromagnet $YbMgGaO_4$, Phys. Rev. Lett. **117**, 097201 (2016).
[26] Y. Shen *et al.*, Evidence for a spinon Fermi surface in a triangular-lattice quantum-spin-liquid candidate, Nature (2016).
[27] J. A. M. Paddison, M. Daum, Z. L. Dun, G. Ehlers, Y. H. Liu, M. B. Stone, H. D. Zhou, and M. Mourigal, Continuous excitations of the triangular-lattice quantum spin liquid $YbMgGaO_4$, Nat. Phys. (2016).
[28] Y. D. Li, X. Q. Wang, and G. Chen, Anisotropic spin model of strong spin-orbit-coupled triangular antiferromagnets, Phys. Rev. B **94**, 035107 (2016).

[29] C. P. Nave and P. A. Lee, Transport properties of a spinon Fermi surface coupled to a U(1) gauge field, Phys. Rev. B **76**, 235124 (2007).

[30] M. Sutherland *et al.*, Thermal conductivity across the phase diagram of cuprates: Low-energy quasiparticles and doping dependence of the superconducting gap, Phys. Rev. B **67**, 174520 (2003).

[31] S. Y. Li, J. B. Bonnemaison, A. Payeur, P. Fournier, C. H. Wang, X. H. Chen, and L. Taillefer, Low-temperature phonon thermal conductivity of single-crystalline Nd_2CuO_4: Effects of sample size and surface roughness, Phys. Rev. B **77**, 134501 (2008).

[32] S. S. Lee and P. A. Lee, U(1) Gauge Theory of the Hubbard Model: Spin-Liquid States and Possible Application to κ-$(BEDT\text{-}TTF)_2Cu_2(CN)_3$, Phys. Rev. Lett. **95**, 036403 (2005).

[33] D. F. Mross, J. McGreevy, H. Liu, and T. Senthil, Controlled expansion for certain non-Fermi-liquid metals, Phys. Rev. B **82**, 045121 (2010).

[34] H. Freire, Controlled calculation of the thermal conductivity for a spinon Fermi surface coupled to a U(1) gauge field, Ann. Phys. (Amsterdam) **349**, 357 (2014).

[35] M. Yamashita, T. Shibauchi, and Y. Matsuda, Thermal-transport studies of two-dimensional quantum spin liquids, Chem. Phys. Chem. **13**, 74 (2012).